

Dimers of and Tautomerism between 2-Pyrimidinethiol and 2(1*H*)-Pyrimidinethione: A Density Functional Theory (DFT) Study

Fillmore Freeman*

Department of Chemistry, University of California, Irvine, Irvine, California 92697-2025

Henry N. Po

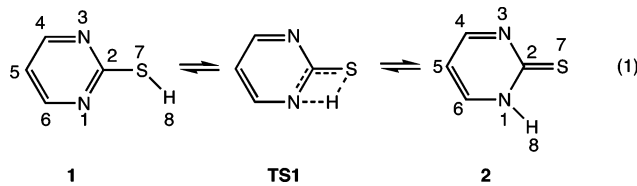
Department of Chemistry and Biochemistry, California State University, Long Beach, Long Beach, California 90840

Received: January 3, 2006

Density functional theory (BLYP, B3LYP, B3P86, B3PW91) with the 6-31+G(d,p), 6-311+G(d,p), and cc-pVTZ basis sets has been used to calculate structural parameters, relative energies, and vibrational spectra of 2-pyrimidinethiol (**1**) and 2(1*H*)-pyrimidinethione (**2**) and their hydrogen-bonded homodimers (*C*₂ **3**, *C*_{2h} **4**[‡], **5**), monohydrates, and dihydrates and a heterodimer (**6**). Several transition state structures proposed for the tautomerization process have also been examined. At the B3PW91/6-311+G(d,p)//B3PW91/6-31+G(d,p) level of theory 2-pyrimidinethiol (**1**) is predicted to be 3.41 kcal/mol more stable (*E*_{rel}) than 2(1*H*)-pyrimidinethione (**2**) in the gas phase and **2** is predicted to be 6.47 kcal/mol more stable than **1** in aqueous medium. An unfavorable planar intramolecular strained four center transition state (**TS1**) for the tautomerization of **1** and **2** in the gas-phase lies 29.07 kcal/mol higher in energy than 2-pyrimidinethiol (**1**). The *C*₂ 2-pyrimidinethiol dimer (**3**) is 6.84 kcal/mol lower in energy than the *C*₂ homodimer transition state structure ([**11**][‡]) that connects dimers **3** and **4**. Transition state [**11**][‡] provides a facile pathway for tautomerization between **1** and **2** in the gas phase (monomer–dimer promoted tautomerization). The hydrogen bonded 2-pyrimidinethiol- - H₂O and 2-pyrimidinethiol- - 2H₂O structures are predicted to be 1.27 and 1.55 kcal/mol, respectively, higher in energy than 2(1*H*)-pyrimidinethione- - H₂O and 2(1*H*)-pyrimidinethione- - 2H₂O. Water promoted tautomerization via cyclic transition states involving one water molecule (**TS**- - H₂O, [**12**][‡]) and two water molecules (**TS**- - 2H₂O, [**13**][‡]) lie 11.42 and 11.44 kcal/mol, respectively, higher in energy than 2-pyrimidinethiol- - H₂O and 2-pyrimidinethiol- - 2H₂O. Thus, the hydrated transition states [**12**][‡] and [**13**][‡] are involved in the tautomerism between **1** and **2** in aqueous medium.

Introduction

Tautomerism (eq 1), dimer formation, hydrated structures, and hydrogen bonds in heterocycles play significant roles in medicine,^{1,2} biochemistry, and chemical systems.^{3–9} Pyrimidinethiols and their derivatives have been used in surface chemistry and coordination chemistry because of the binding capability of nitrogen and sulfur to metals.^{4–9} Owing to their applications in many fields, 2-pyrimidinethiol (2-mercaptopurine, **1**) and its tautomer 2(1*H*)-pyrimidinethione (2-pyrimidinethione, **2**) have been widely studied.^{1–15} Both **1** and **2** can also exist as homodimers (*C*₂ **3**, Figure 2; *C*_{2h} **4**[‡], *C*_{2h} **5**) and as heterodimers (e.g., **6**) in the gas phase, in solution, and in metal complexes. Transition state **TS1** has been implicated in the tautomerization between **1** and **2** in the gas phase (eq 1).



Experimental studies of the vibrational spectra of pyrimidinethiols have been reported,^{12–15} but there does not appear to be any computational or spectroscopic studies on their respective hydrogen bonded dimers and hydrates, or on the possible transition states involved in their tautomeric interconversion. There are only a few computational studies on **1** and **2** [CND0/

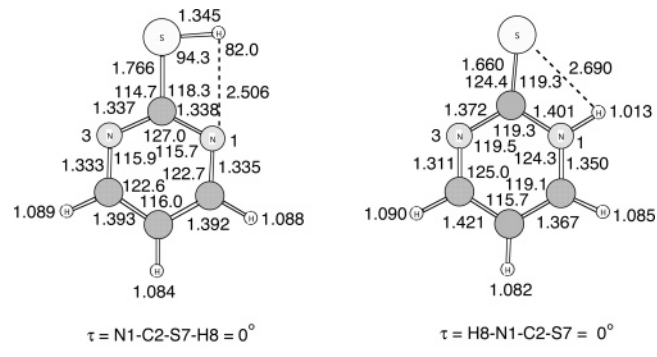


Figure 1. B3PW91/6-31+G(d,p) optimized geometries for 2-pyrimidinethiol (**1**) and 2(1*H*)-pyrimidinethione (**2**).

2,¹⁰ MNDO,¹¹ HF/3-21G(d),¹² MBPT(2)/6-31G(d),¹² and UB-PW91/6-31+G(d,p)].⁹ This report presents the results of density functional theory (BLYP, B3P86, B3LYP, B3PW91) calculations with the 6-31+G(d,p), 6-311+G(d,p), and cc-pVTZ basis sets of the vibrational spectra, structural parameters, and relative energies of 2-pyrimidinethiol (**1**) and 2-pyrimidinethione (**2**) and their homodimers (**3**, **4**[‡], and **5**), heterodimer (**6**), monohydrates (**7**, **8**) and dihydrates (**9**, **10**). Solvent effects and transition states involved in the mechanism of tautomerism between **1** and **2** are also included. To increase the confidence of these results, when possible, the relationships between available experimental data, our computational studies, and the computational predictions of others are compared.

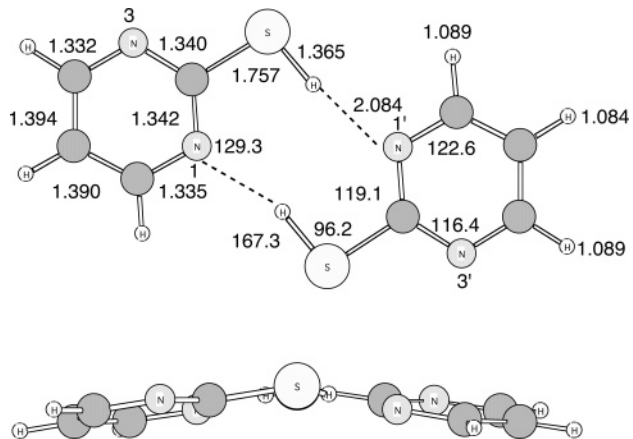


Figure 2. B3PW91/6-31+G(d,p) optimized structure, including side-view, for the C_2 2-pyrimidinemethiol dimer (**3**). Dihedral angles = $\tau = N1-C2-N1'-C2' = 16.6^\circ$, $\tau = C2-S7-C2'-S7' = 16.9^\circ$, $\tau = N1-C2-S7-H8 = \tau = N1'-C2'-S7'-H8' = 3.7^\circ$.

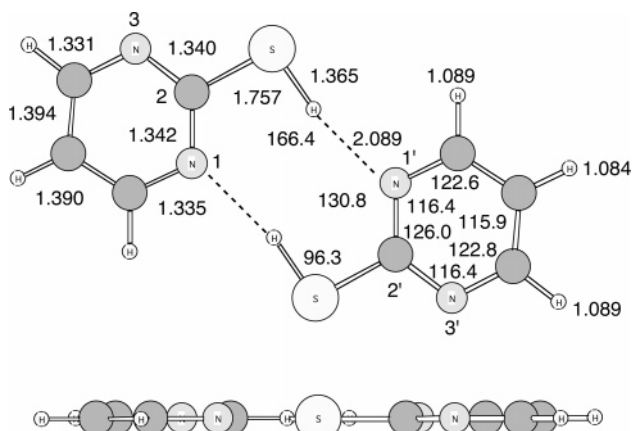


Figure 3. B3PW91/6-31+G(d,p) optimized structure, including side-view, for the C_{2h} 2-pyrimidinemethiol dimer transition state [4] ‡ . Dihedral angles = $\tau = N1-C2-N1'-C2' = \tau = C2-S7-C2'-S7' = \tau = N1-C2-S7-H8 = \tau = N1'-C2'-S7'-H8' = 0^\circ$.

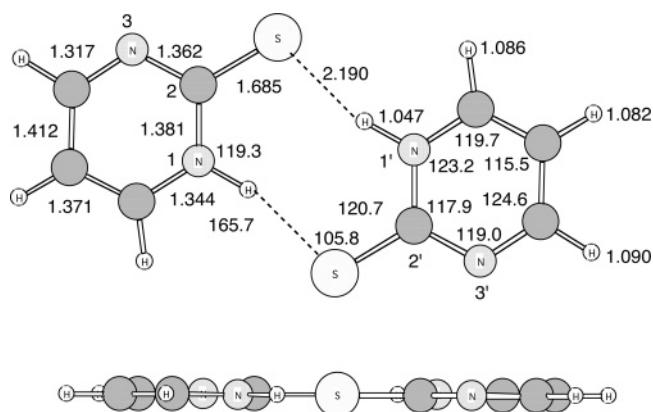


Figure 4. B3PW91/6-31+G(d,p) optimized structure, including side-view, for the C_{2h} 2(1H)-pyrimidinemethiol (**5**). Dihedral angles = $\tau = N1-C2-N1'-C2' = C2-S7-C2'-S7' = H-N1-C2-S7 = H'-N1'-C2'-S7' = 0^\circ$.

Theoretical Methods

The calculations were carried out with the Spartan '04 Macintosh,¹⁶ Spartan '02 Unix,¹⁶ and Gaussian 03^{17a,b} computational programs. Geometry optimizations of all structures were carried out with the DFT models and the 6-31+G(d,p) basis set and single point energy calculations on the optimized structures were obtained with the 6-311+G(d,p) and cc-pVTZ

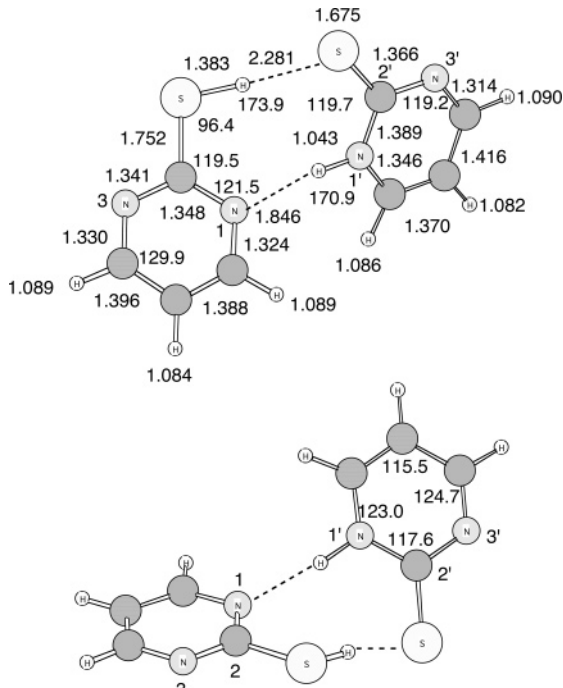


Figure 5. Two views of the B3PW91/6-31+G(d,p) optimized structure of the 2-pyrimidinemethiol-2(1H)-pyrimidinemethiol heterodimer (**6**). Dihedral angles = $\tau = N1-C2-S7-H8' = 15.9^\circ$, $\tau = H8-N1'-C2'-S7' = 4.7^\circ$, $\tau = N1-C2-N1'-C2' = 125.8^\circ$, and $\tau = C2-S7-C2'-S7' = 120.7^\circ$.

basis sets. The 6-311+G(d,p) basis set is of triple- ζ quality for valence electrons^{16c} and basis sets with diffuse functions are useful for calculations of anions and structures with lone pairs.^{17bc} The Dunning's correlation consistent triple- ζ basis set is cc-pVTZ.¹⁸ DFT provides electron correlation which acts to reduce overall charge separation^{16b} and is useful in conformational studies.¹⁹ BLYP is a pure functional^{20–23} while B3LYP,^{20,21,24–26} B3P86,²⁷ and B3PW91^{26,28,29} are hybrid functionals.

The geometries were optimized using BLYP, B3LYP, B3P86, and B3PW91 with the 6-31+G(d,p) basis set. No constraints were imposed on the structures in the equilibrium geometry calculations and in the transition state structure optimizations. Vibrational frequency analyses were carried out on the optimized structures in order to assess the nature of the stationary points and to obtain zero point vibrational energies (ZPVE). The characteristics of local minima and transition states were verified by establishing that the matrices of the energy second derivatives (Hessians) have either zero (number of imaginary frequencies NIMAG = 0) or one negative eigenvalue (NIMAG = 1), respectively.

The single point energy calculations were carried out on the geometry optimized structures. The relative energy (E_{rel}) is the difference in calculated energy without ZPVE or other corrections. The $H(0)_{\text{rel}}$ is the difference in enthalpy at 0 K ($H(0)_{\text{rel}} = E_{\text{rel}} + \text{ZPVE}$ correction), which is also the difference in free energy [$G(0)_{\text{rel}}$] at that temperature. $H(298)_{\text{rel}}$ and $G(298)_{\text{rel}}$ are the enthalpy and free energy differences corrected to 298 K. The BLYP, B3LYP, B3P86, and B3PW91 frequencies were scaled by 0.9940, 0.9613, 0.9914, and 0.9573, respectively. The zero point vibrational energies (ZPVE) for BLYP and B3LYP were scaled by 1.0119 and 0.9804, respectively, in the calculations of the relative thermodynamic parameters.^{17b,30,31}

Aqueous solvation energies were obtained using the SM5.4/A procedure of Cramer and Truhlar³² and the self-consistent reaction field (SCRF) Tomasi polarized continuum model

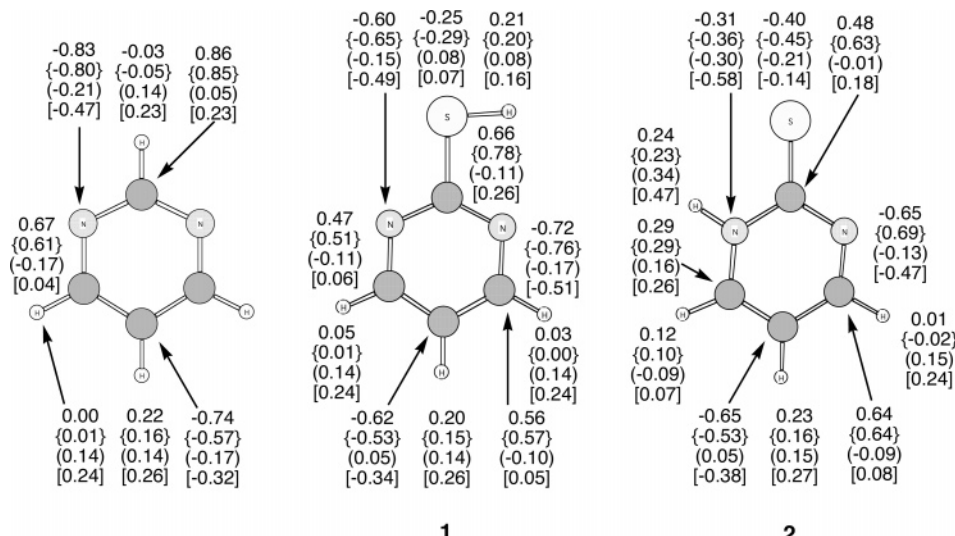


Figure 6. B3PW91/6-31+G(d,p) partial atomic charges for pyrimidine, 2-pyrimidinethiol (**1**), and 2(1*H*)-pyrimidinethione (**2**): MKS, CHelpG{ }, Mulliken (), NPA [].

(PCM).³³ Transition states were located using the linear synchronous transit method,¹⁶ the synchronous transit-guided quasi-Newton (STQN) QST2 or QST3 method,^{17a} and the Berny algorithm.^{17a} Intrinsic reaction coordinate (IRC) calculations in which the imaginary mode for the transition state is followed in both the forward and reverse directions were used to connect the transition states to their respective minima.³⁴

The van der Waals radii of 1.20, 1.55, and 1.80 Å are used for hydrogen, nitrogen, and sulfur, respectively.³⁵ Total energies are in atomic units (au) and the other energies are in kcal/mol. Throughout this paper bond angles and torsional (dihedral) angles are in deg, bond lengths are in angstroms (Å), dipole moments (μ) are given in debyes (D), atomic charges are given in electrons, and entropies are given in cal/mol·K.

Results and Discussion

It is known that computational studies of sulfur-containing compounds often show large basis set effects.^{36–40} Our calculations on these structures with HF and MP2 methods were not as consistent as those from density functional theory (DFT). In this study the DFT hybrid functionals B3LYP, B3P86, and B3PW91 gave similar predictions of molecular parameters and relative energies and the results from B3P86 and B3PW91 were overall the most consistent and efficacious. The usefulness of B3PW91 to describe the tautomeric equilibrium of 4,6-dimethyl-2-mercaptopurine in solution has been reported,^{15a} and it has also been observed that B3PW91 performs much better than BLYP and B3LYP in a study of the interaction energies of van der Waals and hydrogen bonded systems.⁴¹ B3LYP was recommended over HF and MP2 in a study of the molecular structure and vibrational IR spectra of tautomers of 2-pyridinethiol and its hydroxy and seleno analogues.⁴² However, DFT was not recommended for computing the relative energies of thiol/thione tautomeric systems with small energy differences ($E_{\text{rel}} = <3$ kcal/mol), but was recommended for systems with relatively large tautomerization energies ($E_{\text{rel}} = >8$ kcal/mol).^{36,43}

Although crystal structure data are not available for the planar tautomers **1** (C_s , $\mu = 2.88$ D, $E_{\text{aqsolv}} = -9.24$ kcal/mol) and **2** (C_s , $\mu = 7.10$ D, $E_{\text{aqsolv}} = -21.11$ kcal/mol), infrared and Raman spectroscopy confirmed that the 2-pyrimidinethione tautomer (**2**) dominates in the solid state.^{11,12,14,15} The DFT models predict similar geometrical parameters for 2-pyrimidinethiol (**1**) and 2-pyrimidinethione (**2**, Figure 1). The C–S bond in **1** is shorter

than that predicted for 2-pyridinethiol (1.772 Å)^{36,37} and the S7–H8 bond in **1** is longer than that predicted for 2-pyridinethiol (1.332 Å).^{36,37} The C=S bond length in **2** is close to that from the X-ray and neutron diffraction data⁴⁴ and predicted values for 2-pyridinethione (1.665 Å).^{36,37} The N1–C2–S7–H8 dihedral angle in **1** is 0° as is the H8–N1–C2–S7 dihedral angle in **2**.

The distribution of atomic charges is of interest in nonbonding interactions and hydrogen bonds. Several types of methods, each with many possible variations, are widely employed to assign atomic charges.^{16b} The partial atomic charges of 1,3-diazabenzene (pyrimidine), 2-pyrimidinethiol (**1**), and 2-pyrimidinethione (**2**) using the Mulliken population analysis,⁴⁵ natural population analysis phase (NPA) of the natural bond orbital analysis (NBO),⁴⁶ electrostatic potential-derived charges using the CHelpG scheme of Breneman and Wiberg,⁴⁷ and the electrostatic potential-derived charges using the Merz–Kollman–Singh scheme (MKS)⁴⁸ are shown in Figure 6. It is seen that the generated potential derived charges for the MKS and CHelpG models are similar and that their partial atomic charges on the rings are more influenced by the replacement of hydrogen on pyrimidine with a sulfanyl group (SH) than are the Mulliken and NPA models. It is known that the Mulliken population analysis may fail when extended basis and diffuse functions are used (e.g., the partial atomic charge on C4 in pyrimidine is -0.17) and that the NPA leads to exaggerated C–H bond dipoles (Figure 6).

An electrostatic interaction between the nitrogen (N1) and the thiol hydrogen (H8) in 2-pyrimidinethiol (**1**) is reasonable since the optimized N1–H8–S7 intramolecular separation is smaller than the sum of the van der Waals radii for hydrogen and nitrogen (Figure 1).^{35,49} Similarly, an attractive electrostatic interaction between N1–H8 and sulfur in **2** is reasonable since the N1–H8–S7 nonbonded distance is less than the sum of the van der Waals radii for hydrogen and sulfur.

It is difficult to obtain experimental spectra for monomers **1** and **2** owing to the ease of tautomerization and to the sensitivity of **1** to redox reactions. Thus, computational chemistry is especially useful for calculating the spectra of tautomers of heterocycles. This aspect of the discussion is primarily concerned with the vibrational frequencies that can be used to differentiate between tautomers **1** and **2**. This point is important as the relative intensity of the bands can be used to determine

TABLE 1: Relative Energies for 2-Pyrimidinethiol (1**) and 2(1*H*)-Pyrimidinethione (**2**)^{a,b}**

level	<i>E</i> _{rel}
BLYP/6-31+G(d,p)	2.45
BLYP/6-311+G(d,p)	2.50
BLYP/cc-pVTZ	2.90
B3P86/6-31+G(d,p)	2.97
B3P86/6-311+G(d,p)	3.28
B3P86/cc-pVTZ	3.46
B3LYP/6-31+G(d,p)	3.42
B3LYP/6-311+G(d,p)	3.58
B3LYP/cc-pVTZ	3.89
B3PW91/6-31+G(d,p)	3.07
B3PW91/6-311+G(d,p)	3.41
B3PW91/cc-pVTZ	3.60

^a 6-31+G(d,p) optimized structure. ^b *E*_{rel} to thiol = *E*(thione) – *E*(thiol).

TABLE 2: Relative Energies of 2-Pyrimidinethiol (1**), 2(1*H*)-Pyrimidinethione (**2**), and Transition State TS1^{a,b,c}**

structure	<i>E</i> _{rel}	<i>H</i> (0) _{rel}	<i>H</i> (298) _{rel}	<i>G</i> (298) _{rel}
BLYP/6-311+G(d,p)				
1	0.00			
2	2.50	4.44	4.35	4.29
TS1	27.55	25.70	24.85	25.18
B3LYP/6-311+G(d,p)				
1	0.00			
2	3.60	5.61	5.50	5.53
TS1	30.63	28.88	28.62	28.98
B3P86/6-311+G(d,p)				
1	0.00			
2	3.28	5.33	5.22	5.24
TS1	28.90	27.13	26.88	27.22
B3PW91/6-311+G(d,p)				
1	0.00			
2	3.41	5.47	5.36	5.38
TS1	29.07	27.30	27.05	27.40

^a 6-31+G(d,p) optimized structure. ^b *E*_{rel} to thiol = *E*(thione) – *E*(thiol). ^c *E*_{rel} to thiol = *E*_{TS1} – *E*_{thiol}.

experimentally the **1:2** concentration and, assuming a Boltzmann distribution, the energy difference between the tautomers. The peak in the 3055 cm⁻¹ region is characteristic for C–H stretching in the pyrimidine ring. The 2-pyrimidinethiol tautomer (**1**) has the distinctive *v*_{S–H} stretching frequency in the 2600 cm⁻¹ region and 2-pyrimidinethione (**2**) shows the *v*_{N–H} stretching frequency in the 3400 cm⁻¹ region. The band in the 2600 cm⁻¹ region and the band in the 3400 cm⁻¹ region are sufficiently different and can be used to differentiate between the tautomeric species **1** and **2**. The band near 2520 cm⁻¹, which is strongly hydrogen bonded, is assigned to the N1–H8 stretching in 2-pyrimidinethione (**2**). The C=S stretching and N1–H8 out-of-plane deformation are observed in the 1213 cm⁻¹ region and the 1053 cm⁻¹ region, respectively. However, there has been considerable discussion and conflicting reports concerning the locations of the C–S and C=S stretching frequencies.^{8,12,14,15,50} In compounds containing a C=S group adjacent to a C–N or C–O group, there may be interactions between the stretching vibrations of the groups that may produce new frequencies in unexpected regions of the spectrum.^{50b}

It is seen in Tables 1 and 2 and in SI Table 1 in the Supporting Information (SI) that all levels of theory predict the less polar 2-pyrimidinethiol (**1**) to be more stable than 2-pyrimidinethione (**2**) in the gas phase. The cc-pVTZ basis set generally gave larger values of *E*_{rel} than the 6-311+G(d,p) basis set. It is also seen that the pure functional BLYP predicted smaller *E*_{rel} values for **1** and **2** than the hybrid density functionals. At the B3PW91/6-311+G(d,p)/B3PW91/6-311+G(d,p) level of theory the thiol tautomer (**1**) is predicted to be 3.41 kcal/mol more stable than the thione form (**2**). The greater strength of the hydrogen bond

TABLE 3: Relative Energies of 2-Pyrimidinethiol *C*₂ Dimer (3**), 2-Pyrimidinethiol *C*_{2h} Dimer [**4**]^d, 2(1*H*)-Pyrimidinethione *C*_{2h} Dimer (**5**), Heterodimer (**6**), and *C*₂ Dimer Transition State [**11**]^{e,f,g}**

structure	<i>E</i> _{rel}	<i>H</i> (0) _{rel}	<i>H</i> (298) _{rel}	<i>G</i> (298) _{rel}
BLYP/6-311+G(d,p)				
5	0.00			
[4] ^d	6.39 ^c	2.58	2.34	3.98
6	5.11 ^d	2.02	2.63	2.73
B3LYP/6-311+G(d,p)				
5	0.00			
[4] ^d	5.30 ^c	1.37	1.14	2.36
6	5.07 ^d	5.02	2.57	2.08
B3P86/6-311+G(d,p)				
5	0.00			
3	6.43 ^b	2.65	2.33	1.97
[4] ^d	2.95 ^c	2.65	4.57	2.95
6	5.47 ^d	3.49	2.95	3.29
[11] ^d	12.63 ^e	6.05	5.16	7.13
[11] ^d	6.20 ^f	3.40	2.83	5.16
B3PW91/6-311+G(d,p)				
5	0.00			
3	6.27 ^b	2.42	2.14	0.98
[4] ^d	6.27 ^c	2.42	2.16	3.64
6	5.41 ^d	3.44	2.92	2.93
[11] ^d	13.11 ^e	6.43	5.55	7.22
[11] ^d	6.84 ^f	4.10	3.41	6.24

^a 6-31+G(d,p) optimized structure. ^b *E*_{rel} to thione dimer = *E*₃ – *E*₅. ^c *E*_{rel} to thione dimer = *E*_{[4]‡} – *E*₅. ^d *E*_{rel} to thione dimer = *E*₆ – *E*₅. ^e *E*_{rel} to thione dimer = *E*_{[11]‡} – *E*₅. ^f *E*_{rel} to thiol dimer = *E*_{[11]‡} – *E*₃.

to nitrogen in **1** relative to the hydrogen bond to sulfur in **2** contributes to the greater stability of **1**. In contrast to the gas phase predictions, in aqueous medium, the thione tautomer (**2**) is favored by 8.80 kcal/mol over the thiol form (**1**). Although 2-pyrimidinethiol (**1**) and 2-pyrimidinethione (**2**) are stabilized by electron delocalization and thioamide resonance in the gas phase, it is reasonable to expect a differential solvent stabilization in polar media owing in part to the larger dipole moment of **2**. Thus, 2-pyrimidinethione (**2**) is stabilized more than **1** in polar solvents owing to its dipolar structure and to thioamide resonance.

The 2-pyrimidinethiol (**1**) D 2-pyrimidinethione (**2**) tautomeric equilibrium (eq 1) is also influenced by homodimer (**3**, [**4**]^d, **5**) and heterodimer formation (**6**) and by the redox chemistry of **1** and its disulfide. The four levels of theory located the *C*_{2h} thione dimer (**5**, $\mu = 0$ D, Figure 4), which is a minimum, but only B3P86 and B3PW91 located the *C*₂ thiol dimer (**3**, $\mu = 1.47$ D, Figure 2). The *C*₂ thiol dimer (**3**) is a minimum (no imaginary vibrational frequency), and the *C*_{2h} 2-pyrimidinethiol dimer ([**4**]^d, $\mu = 0$ D, Figure 3) has one imaginary vibrational frequency (10*i* cm⁻¹). All levels of theory predict the *C*_{2h} thione dimer (**5**) to be more stable than the *C*₂ thiol dimer (**3**, *E*_{rel} = 6.27 kcal/mol, Table 3 and SI Table 2), [**4**]^d (*E*_{rel} = 6.27 kcal/mol, Table 4 and SI Table 3), and the heterodimer (**6**, *E*_{rel} = 5.07 kcal/mol, Table 3 and SI Tables 3 and 5) in the gas phase. The *C*₂ thiol dimer (**3**) is only slightly more stable than the *C*_{2h} thiol dimer ([**4**]^d, *E*_{rel} = 0.30 kcal/mol) and has a lower symmetry and different dihedral angles (Figures 2 and 3) than [**4**]^d (N1–C2–S7–H8 = N1'–C2'–S7'–H8' = 0°). The thiol *C*₂ dimer (**3**) also has a lower symmetry and different torsional angles than the *C*_{2h} 2-pyrimidinethione dimer (**5**). The heterodimer (**6**, Figure 5) is slightly more stable than the *C*₂ thiol dimer (**3**, *E*_{rel} = 0.86 kcal/mol, Table 3, SI Table 4) and is significantly more polar ($\mu = 8.82$ D) than either dimer **3** or dimer **5**. Selected structural parameters of dimers **3**, [**4**]^d, **5**, and **6** are given in Figures 2–5, respectively. It is seen that the four atoms in the torsional angle N1–C2–S7–H8 in **1**, **3**, **4**, and **5** maintain their planarity ($\tau = 0$ °). Similarly, in **2** and in the *C*_{2h} thione dimer

TABLE 4: Relative Energies of for 2-Pyrimidinethiol- -H₂O (7) and 2(1*H*)-Pyrimidinethione- -H₂O (8)^{a,b}

structure	<i>E</i> _{rel}	<i>H</i> (0) _{rel}	<i>H</i> (298) _{rel}	<i>G</i> (298) _{rel}
		BLYP/6-311+G(d,p)		
7	1.62	-0.30	-0.10	-0.59
8	0.00			
		B3LYP/6-311+G(d,p)		
7	0.97	-1.04	-0.81	-1.38
8	0.00			
		B3P86/6-311+G(d,p)		
7	1.50	-0.42	-0.23	-0.67
8	0.00			
		B3PW91/6-311+G(d,p)		
7	1.27	-0.71	-0.50	-1.01
8	0.00			

^a 6-31+G(d,p) optimized structure. ^b *E*_{rel} to **8** = *E*₇ - *E*₈. ^c *E*_{rel} to thiol = *E*_{Ts1} - *E*_{thiol}.

TABLE 5: Relative Energies of 2-Pyrimidinethiol- -2H₂O (9) and 2(1*H*)-Pyrimidinethione- -2H₂O (10)^{a,b}

structure	<i>E</i> _{rel}	<i>H</i> (0) _{rel}	<i>H</i> (298) _{rel}	<i>G</i> (298) _{rel}
		BLYP/6-311+G(d,p)		
9	3.70	1.73	1.90	1.54
10	0.00			
		B3LYP/6-311+G(d,p)		
9	3.20	1.17	1.42	0.98
10	0.00			
		B3P86/6-311+G(d,p)		
9	3.77	1.85	1.99	1.85
10	0.00			
		B3PW91/6-311+G(d,p)		
9	3.54	1.55	1.71	1.34
10	0.00			

^a 6-31+G(d,p) optimized structure. ^b *E*_{rel} to **10** = *E*₉ - *E*₁₀.

(5), the H8-N1-C2-S7 and H8'-N1'-C2'-S7' dihedral angles are 0°. In contrast, in the heterodimer **6** the torsional angles N1-C2-S7-H8 and H8'-N1'-C2'-S7' are 14.1 and 4.0°, respectively, which reflect twisting in the structure (Figure 5).

The predicted S7-H8 vibrational frequency in the *C*₂ thiol dimer (**3**) is lowered to the 2383–2404 cm⁻¹ region, indicating lengthening of the S7-H8 bond due to the H8-N1' intramolecular interaction. Vibrational frequency calculations for the *C*_{2h} thione dimer (**5**) predicted neither a S-H stretching frequency in the 2600 cm⁻¹ region nor a N-H stretching frequency in the 3400 cm⁻¹ region. The C2-S7 bond in the *C*₂ thiol dimer (**3**) is 1.757 Å, the S7-H8 bond is 1.365 Å, and the weak nonbonded interaction distance of H8 with N1' of the second pyrimidine ring is 2.084 Å. The corresponding distances C2=S7, S7- -H8, and H8- -N1' for the *C*_{2h} thione dimer (**5**) are 1.685, 2.190, and 1.047 Å, respectively. The C2-N1-H8' angle in dimer **3** is 129.3° and in **5** it is 119.3° suggesting sp² hybridization character at N1 in **5**. The C2-S7-H8 bond angle in **3** is 96.2° which is close to the 94.3° angle in 2-pyrimidinethiol (**1**). In the thiol dimer **3**, the C2-S7-C2'-S7' torsional angle is 16.9° and in the *C*_{2h} thione dimer (**5**), C2-S7-H8 is 105.8° and the dihedral angle for the H atom bridged S7-C2-N1-H8' is 0°, which is consistent with *C*_{2h} symmetry (Figure 4).

In the gas phase, the DFT energy difference (*E*_{rel}) for the dimerization of 2-pyrimidinethiol (**1**) to the *C*₂ thiol dimer (**3**) is 4.62 kcal/mol which reflects in part the respective hydrogen bonds S7-H8- -N1' and S7'-H8'- -N1'. Since electrostatic considerations dominate for most hydrogen bonds, the geometry of the hydrogen bond is not a major factor to strength. However, the optimal hydrogen bond geometry has a collinear arrangement

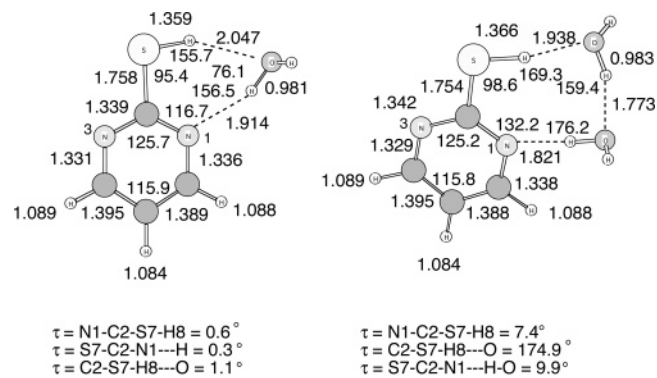


Figure 7. B3PW91/6-31+G(d,p) optimized geometry for 2-pyrimidinethiol- -H₂O (**7**) and 2-pyrimidinethiol 2H₂O (**9**).

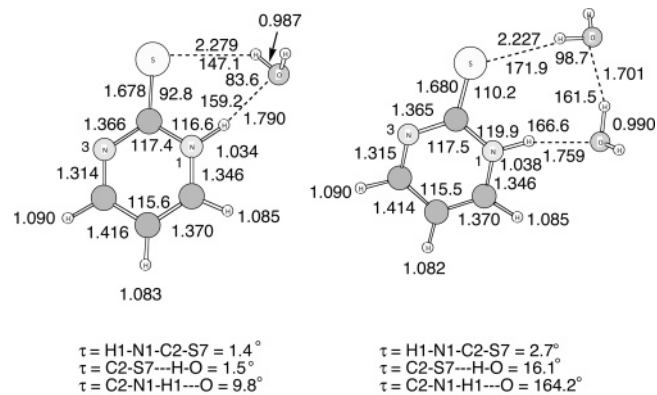


Figure 8. B3PW91/6-31+G(d,p) optimized geometry for 2(1*H*)-pyrimidinethione- -2H₂O (**8**) and 2(1*H*)-pyrimidinethione- -2H₂O (**10**).

of the three atoms. The *E*_{rel} between the monomeric thione **2** and the *C*_{2h} thione dimer (**5**) is 17.72 kcal/mol. This larger stabilization of *C*_{2h} dimer (**5**) is due to dipole–dipole interactions between a pair of thiones because of the dipolar property of thione **2** in addition to hydrogen bonding at N1-H8- -S7' and N1'-H8'- -S7. Unlike the symmetrical dual hydrogen bonding in the dimers **3** and **5**, unsymmetrical dual hydrogen bonding is expected in the heterodimer (**6**, Figure 5). The predicted N1'-H8'- -N1 nonbonded distance in **6** is ~0.44 Å shorter than the C=S7- -H8 distance. The large difference in the hydrogen bonding distances in **6** may be the result of the required unfavorable geometry in forming the dimer and to the fact that the thiocarbonyl group is not strongly polarized since the electronegativities of carbon and sulfur are about the same. It is also seen in Figures 2–5 that the heterodimer **6** has a better collinear arrangement of the three atoms involved in the hydrogen bonding than dimers **3**, [4][‡], or **5**. Thus, unlike the hydrogen bonding in the 2-hydroxypyridine/2-pyridone system, the N1'-H8'- -N1 and S7-H8- -S7' hydrogen-bonding angles in **6** are larger than those in dimer **3** and in dimer **5**⁵⁴ and in some thymine and uracil systems.⁵⁵

It is seen in Figure 7 that the S7-H8- -O hydrogen-bonded distance (2.047 Å) in 2-pyrimidinethiol- -H₂O (thiol- -H₂O, **7**) is longer than that in 2-pyrimidinethione- -2H₂O (thione- -2H₂O, **9**, 1.938 Å) and that the O-H- -N hydrogen bonded distance in (thiol- -H₂O, **7**, 1.914 Å) is longer than that in (thiol- -2H₂O, **9**, 1.821 Å). A similar pattern is observed with the hydrogen bonds in 2-pyrimidinethione- -H₂O (thione- -H₂O, **8**) and 2-pyrimidinethione- -2H₂O (thione- -2H₂O, **10**, Figure 8). In both cases, the hydrogen bonds in the two-water structures are closer to linearity than the angles in the one-

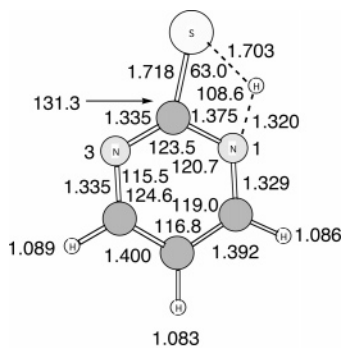


Figure 9. B3PW91/6-31+G(d,p) optimized geometry for transition state **TS1**.

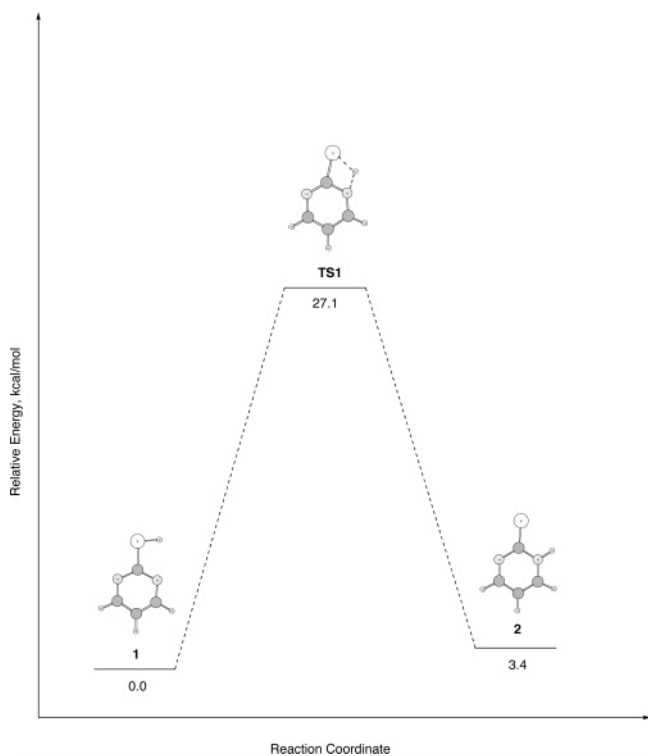


Figure 10. B3PW91/6-31+G(d,p)//B3PW91/6-31+G(d,p) relative energies for 2-pyrimidinethiol (**1**) 2(*H*)-pyrimidinethione (**2**), and transition state **TS1** in the gas phase.

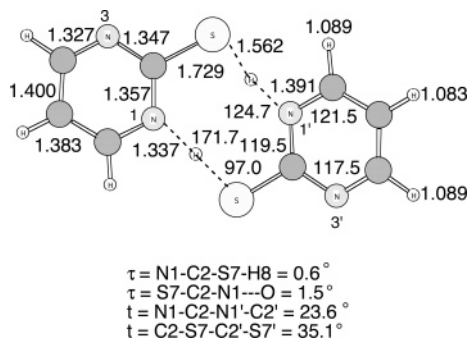


Figure 11. B3PW91/6-31+G(d,p) optimized structure for the 2-pyrimidinethiol C_2 dimer transition state [11][‡].

water structures. Thiol- -H₂O (**7**) and thione- -H₂O (**8**) are relatively close in energy ($E_{\text{rel}} = 1.27 \text{ kcal/mol}$) while the energy difference between thiol- -2H₂O (**9**) and thione- -2H₂O (**10**) is 1.55 kcal/mol (Tables 4 and 5). Thus, the energy differences (E_{rel}) between the thiol and thione one water complexes and

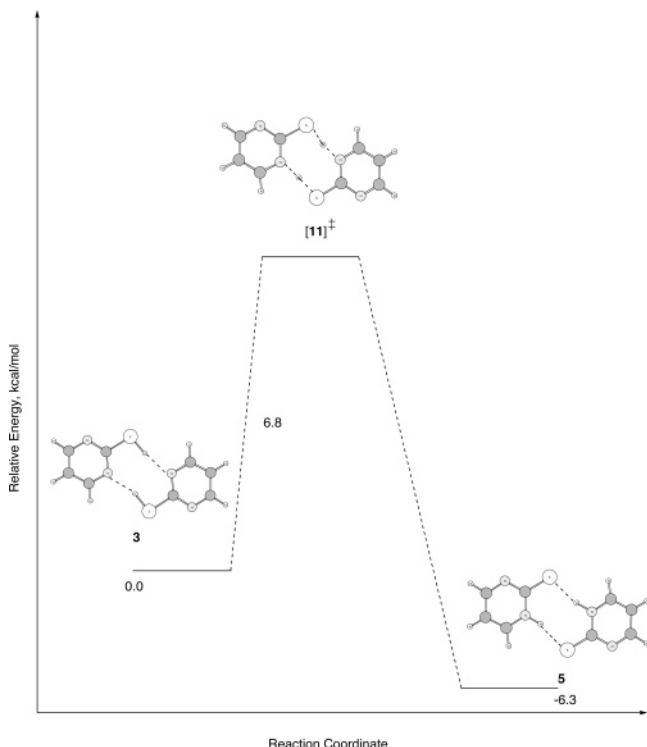


Figure 12. B3PW91/6-311+G(d,p)/B3PW91/6-31+G(d,p) relative energies for the C_2 2-pyrimidinemethol dimer (**3**), C_{2h} 2(1H)-pyrimidinemethione dimer (**5**), and transition state [11][‡] in the gas phase.

the two water complexes are similar. BLYP and B3LYP predicted larger energy differences (E_{rel}) between **9** and **10** than B3P86 and B3PW91 (Table 5). A comparison of Figures 1, 7, and 8 shows that there is little change in the ring geometry in going from the respective monomer to structures with one or two water molecules.

Considering the tautomeric equilibria described above, three types of nondissociative proton-transfer mechanisms for the tautomerization between **1** and **2** in the gas phase, in aprotic medium, and in neutral aqueous solution can be envisaged: (i) an intramolecular proton transfer from sulfur to the pyrimidine ring nitrogen via **TS1** (eq 1); (ii) solvent promoted mechanisms involving one or more water molecules as a bifunctional catalysis via cyclic transition states; (iii) an intermolecular proton transfer within a self-associated dimeric transition state.

Geometrical parameters for transition state **TS1** (eq 1, $\mu = 5.48$ D) are shown in Figure 9. Vibrational frequency calculations show no S–H stretching in the 2600 cm^{-1} region for **TS1** indicating that the S–H bond is essentially broken since it has lengthened from 1.345 to 1.703 Å. The N1–H8 distance (1.320 Å) in **TS1** is shorter than the N1–H8 nonbonded distance in **1** (2.506 Å) and is considerably longer than the N–H bond in **2** (1.013 Å) indicating partial N–H bond formation. In **TS1** as the S7–H8 distance increases from 1.345 Å to 1.703 Å, the H atom moves closer (from 2.506 Å to 1.320 Å) toward the N1 atom of the pyrimidine ring. The C2–S7 bond distance in **TS1** is also shorten from 1.766 to 1.718 Å. These geometrical changes involving the strained four center ring contribute to the relatively high energy barrier of 29.1 kcal/mol between **1** and **TS1** (Table 2). Although, this high energy barrier does not rule out involvement of unfavorable **TS1** in a unimolecular tautomerization process between **1** and **2** in the gas phase (Figure 10), other lower energy paths are available (*vide infra*). The energy difference (E_{rel}) between 2-pyridinethiol and its intramolecular four center transition state is 25 to 30 kcal/mol.^{36,37}

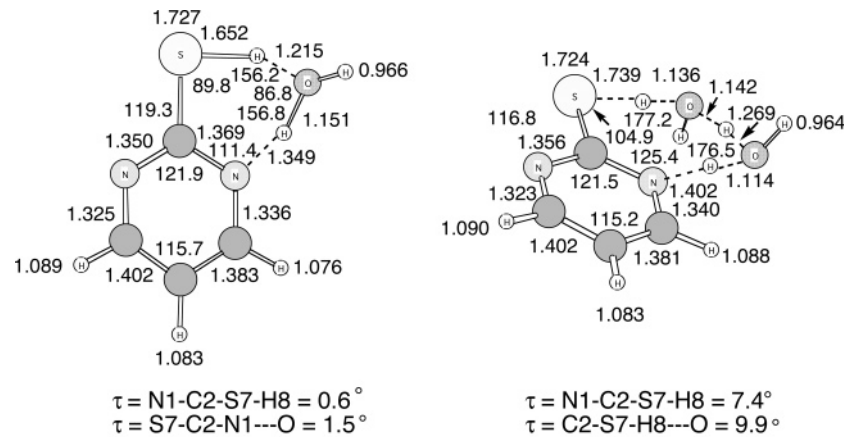


Figure 13. B3PW91/6-31+G(d,p) optimized transition state structures $\text{TS}_{\text{--} \cdots \text{H}_2\text{O}}^{[12]^{\ddagger}}$ and $\text{TS}_{\text{--} \cdots \text{H}_2\text{O}}^{[13]^{\ddagger}}$

TABLE 6: Relative Energies of for
2-Pyrimidinethiol- -H₂O (7) and Transition State TS- -H₂O
[12]^{a,b}

structure	E_{rel}	$H(0)_{\text{rel}}$	$H(298)_{\text{rel}}$	$G(298)_{\text{rel}}$
BLYP/6-311+G(d,p)				
7 [12] [‡]	0.00 11.38	8.97	7.96	10.35
B3LYP/6-311+G(d,p)				
7 [12] [‡]	0.00 14.03	11.68	10.60	13.14
B3P86/6-311+G(d,p)				
7 [12] [‡]	0.00 10.60	8.24	7.28	9.45
B3PW91/6-311+G(d,p)				
7 [12] [‡]	0.00 11.42	9.12	8.10	10.46

BLYP, B3P86, and B3PW91 located the C_2 dimer transition state [11] \ddagger but B3LYP did not. Transition state [11] \ddagger (Figure 1) is 6.84 kcal/mol higher in energy than the C_2 thiol dimer (**3**) and 13.11 kcal/mol lower in energy than the C_{2h} thione dimer (**5**, Table 3). IRC calculations showed that transition state [11] \ddagger connects the C_2 thiol dimer (**3**) and the C_{2h} thione dimer (**5**, Figure 12). Transition state [11] \ddagger , with a barrier of 6.84 kcal/mol, provides a facile pathway for tautomerization between **1** and **2** in the gas phase (monomer–dimer promoted tautomerization).

It is clear that the tautomeric equilibrium in the 2-pyrimidinethiol (**1**) \rightleftharpoons 2-pyrimidinethione (**2**) system is shifted toward the thione form in the presence of water, which suggests that water may also assist in the tautomeric interconversion.^{4a,d,5,8,56–58} This solvent-assisted shift of the tautomeric equilibrium from the thiol form to the thione form is due to the difference in the dipole–dipole and dipole–induced dipole interactions of the respective tautomers with the solvent molecules. Solvent-promoted tautomerization via transition states involving one water molecule (**TS** - - H_2O , **[12] ‡**) and two water molecules (**TS** - - $2\text{H}_2\text{O}$, **[13] ‡** , Figure 13) lie 11.42 and 11.44 kcal/mol, respectively, higher in energy than pyrimidinethiol- - H_2O (**7**) and pyrimidinethiol- - $2\text{H}_2\text{O}$ (**8**, Tables 6 and 7). **TS** - - H_2O [**12] ‡** (Figure 14) and **TS** - - $2\text{H}_2\text{O}$ [**13] ‡** (Figure 15) were shown to connect their respective minima (2-pyrimidinethiol hydrates and 2-pyrimidinethione hydrates) by carrying out intrinsic reaction coordinate (IRC) calculations in which the imaginary modes for the transition states were followed in the forward and reverse directions. Thus, the barrier heights ([**12] ‡ , [**13] ‡])****

TABLE 7: Relative Energies of 2-Pyrimidinethiol- \cdots - $2\text{H}_2\text{O}$ (8) and Transition State TS- \cdots - $2\text{H}_2\text{O}$ [13] $^{\ddagger, a,b}$

structure	E_{rel}	$H(0)_{\text{rel}}$	$H(298)_{\text{rel}}$	$G(298)_{\text{rel}}$
BLYP/6-311+G(d,p)				
8 [13] [‡]	0.00			
	11.84	8.57	7.29	10.30
B3LYP/6-311+G(d,p)				
8 [13] [‡]	0.00			
	14.38	11.40	9.97	13.15
B3P86/6-311+G(d,p)				
8 [13] [‡]	10.21	7.21	9.00	11.64
B3PW91/6-311+G(d,p)				
8 [13] [‡]	11.44	8.53	7.22	10.23

for the solvent assisted tautomerization of **1** and **2** are significantly lower than that involving transition state **TS1** in the gas phase (cf. Figure 10).

Conclusions

Among the functional used in this study, B3P86 and B3PW91 gave the most consistent overall results. All levels of theory (BLYP, B3LYP, B3P86, B3PW91) predict 2-pyrimidinethiol (**1**) to be more stable than 2-pyrimidinethione (**2**) in the gas phase and **2** to be more stable in aqueous medium. The C_{2h} 2-pyrimidinethione dimer (**5**) is predicted to be more stable than the C_2 2-pyrimidinethiol dimer (**3**) in the gas phase and in the aqueous medium.

Owing in part to geometrical deformations, the intramolecular transition state **TS1** with a strained four center ring for the tautomer interconversion of monomeric 2-pyrimidinethiol (**1**) and 2-pyrimidinethione (**2**) lies 29.07 kcal/mol higher than (**1**) in the gas phase. The C_2 2-pyrimidinethiol dimer (**3**) is 6.84 kcal/mol lower in energy than the C_2 dimer transition state (**[11] \ddagger**) that connects thiol dimer **3** and thione dimer **4**. The C_2 dimer transition state (**[11] \ddagger**) provides a facile pathway for tautomerization between **1** and **2** in the gas phase (monomer–dimer promoted tautomerization). 2-Pyrimidinethiol- -H₂O (**7**) and 2-pyrimidinethiol- -2H₂O (**9**) are predicted to be 1.27 and 1.55 kcal/mol, respectively, higher in energy than 2(1*H*)-pyrimidinethione- -H₂O (**8**) and 2(1*H*)-pyrimidinethione- -2H₂O (**10**). Water promoted tautomerization via transition states involving one water molecule (**TS**- -H₂O, **[12] \ddagger**) and two water

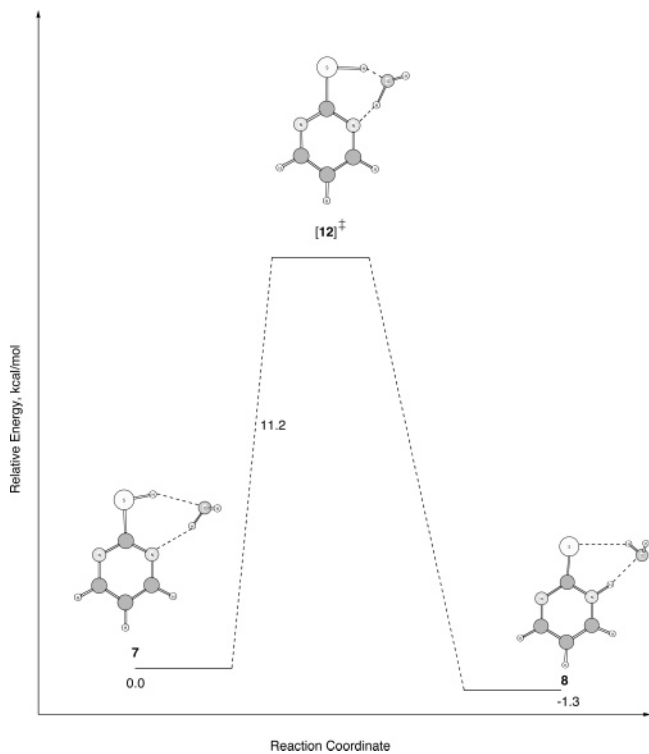


Figure 14. B3PW91/6-311+G(d,p)//B3PW91/6-31+G(d,p) relative energies for the C_2 2-pyrimidinethiol- - H_2O (**7**), C_{2h} 2(1*H*)-pyrimidinethione- - H_2O (**8**), and transition state TS - - H_2O [**12**][‡].

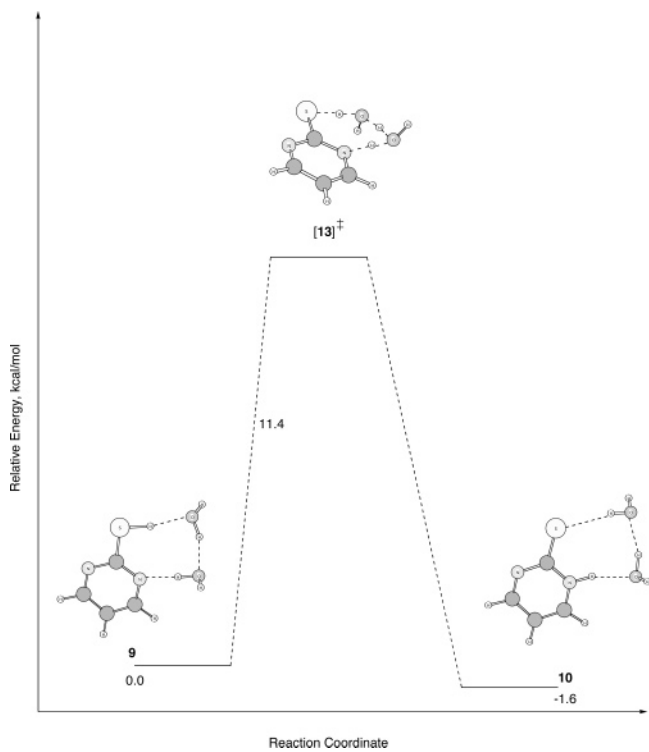


Figure 15. B3PW91/6-311+G(d,p)//B3PW91/6-31+G(d,p) relative energies for 2-pyrimidinethiol- - $2H_2O$ (**9**), 2(1*H*)-pyrimidinethione- - $2H_2O$ (**10**), and transition state TS - - $2H_2O$ [**13**][‡].

molecules (TS - - $2H_2O$, [**13**][‡]) lie 11.42 and 11.44 kcal/mol, respectively, higher in energy than 2-pyrimidinethiol- - H_2O (**7**) and 2-pyrimidinethiol- - $2H_2O$ (**9**).

Supporting Information Available: Tables of equilibrium geometry parameters, relative thermodynamic parameters, and

thermochemical data. This material is available free of charge via the Internet at <http://pubs.acs.org>.

References and Notes

- (a) Morris, D. R.; Hager, L. P. *J. Biol. Chem.* **1966**, *241*, 3582–3589. (b) Taurog, A. *Endocrinology* **1976**, *98*, 1031–1046. (c) Engler, H.; Taurog, A.; Nakashima, T. *Biochem. Pharmacol.* **1982**, *31*, 3801–3806. (d) Ahren, B.; Rerup, C. *Pharmacol. Toxicol.* **1987**, *61*, 69–71. (e) Lindsay, H. R.; Cash, A. G.; Vaughn, A. W.; Hill, J. B. *Biochem. Pharmacol.* **1977**, *26*, 617–623. (f) Bjorstein, F. *Biochim. Biophys. Acta* **1966**, *127*, 265–268.
- (2) Gonzalez, V. M.; Fuertes, M. A.; Perez-Alvarez, M. J.; Cervantes, G.; Moreno, V.; Alonso, C.; Perez, J. M. *Biochem. Pharmacol.* **2000**, *60*, 371–379.
- (3) Toda, F.; Tanaka, K.; Sato, J. *Tetrahedr. Asymm.* **1993**, *4*, 1771–1774.
- (4) (a) Pinheiro, L. S.; Temperini, M. L. A. *Surf. Sci.* **1999**, *441*, 45–52. (b) Pinheiro, L. S.; Temperini, M. L. A. *Surf. Sci.* **1999**, *441*, 53–64. (c) Pinheiro, L. S.; Temperini, M. L. A. *Appl. Surf. Sci.* **2001**, *171*, 89–100. (d) Davis, J. J.; Hill, H. A. O.; Yamada, R.; Naohara, H.; Uosaki, K. *J. Chem. Soc., Faraday Trans.* **1988**, *94*, 1315–1319.
- (5) Pang, Y. S.; Hwang, H. J.; Kim, M. S. *J. Mol. Struct.* **1998**, *441*, 63–76.
- (6) (a) Huber, F.; Schmidgen, R.; Schurmann, M.; Barbieri, R.; Ruisi, G.; Silvestri, A. *Appl. Organomet. Chem.* **1997**, *11*, 869–888. (b) Schmidgen, R.; Huber, F.; Schurmann, M.; Silvestri, A.; Ruisi, G.; Rossi, M.; Barbieri, R. *Appl. Organomet. Chem.* **1998**, *12*, 861–871.
- (7) Contreras, J. G.; Seguel, G. V.; Alderete, J. B. *Spectrochim. Acta* **1994**, *50A*, 371–374.
- (8) (a) Zhang, H.-L.; Evans, S. D.; Henderson, J. R.; Miles, R. L.; Shen, T. *J. Phys. Chem. B* **2003**, *107*, 6087–6095. (b) Zhang, H.-L.; Chen, M.; Li, H.-L. *J. Phys. Chem. B* **2000**, *104*, 28–36.
- (9) Tripathi, G. N. R.; Clements, M. *J. Phys. Chem. B* **2003**, *107*, 11125–11132 and references therein.
- (10) Berndt, M.; Kwiatkowski, J. S.; Budzinski, J.; Szczodrowska, B. *Chem. Phys. Lett.* **1973**, *19*, 246–250.
- (11) Contreras, J. G.; Alderete, J. B. *J. Mol. Struct. (THEOCHEM)* **1991**, *231*, 257–265.
- (12) Nowak, M. J.; Rostkowska, H.; Lapinski, L.; Leszczynski, J.; Kwiatkowski, J. S. *Spectrochim. Acta* **1991**, *47A*, 339–353.
- (13) (a) Dollish, F. R.; Fateley, W. G.; Bentley, F. F. *Characteristic Raman Frequencies of Organic Compounds*; Wiley & Sons: New York, 1974. (b) Lord, R. C.; Marston, A. L.; Miller, F. A. *Spectrochim. Acta* **1957**, *9*, 113–125. (c) Sabrana, G.; Adembris, G.; Califano, S. *Spectrochim. Acta* **1966**, *22*, 1830–1842.
- (14) (a) Sathyaranayana, D. N.; Raja, S. V. K. *Spectrochim. Acta* **1985**, *41A*, 809–813. (b) Shunmugam, R.; Sathyaranayana, D. N. *Bull. Soc. Chim. Belg.* **1984**, *93*, 121–127. (c) Shunmugam, R.; Sathyaranayana, D. N. *Spectrochim. Acta* **1954**, *40A*, 757–761. (d) Goel, R. K.; Gupta, C.; Gupta, S. P. *Indian J. Pure Appl. Chem.* **1985**, *23*, 344–348. (e) Spinner, E. J. *Chem. Soc.* **1960**, 1237. (f) Spinner, E. J. *Org. Chem.* **1958**, *23*, 2037–2308.
- (15) (a) Martos-Calvente, R.; de la Peña O’Shea, V. A.; Campos-Martín, J. M.; Fierro, J. L. G. *J. Phys. Chem. A* **2003**, *107*, 7490–7495. (b) Stoyanov, S.; Petrov, I.; Antonov, L.; Stoyanov, T.; Karagiannidis, P.; Aslanidis, P. *Can. J. Chem.* **1990**, *68*, 1482–1489. (c) Stoyanov, S.; Stoyanov, T.; Akrivos, P. D. *Trends Appl. Spectrosc.* **1998**, *2*, 89–103. (d) Gupta, S. P.; Sharma, S.; Goel, R. K. *Spectrochim. Acta* **1986**, *42A*, 1171–1179.
- (16) (a) Kong, J.; White, C. A.; Krylov, A. I.; Sherrill, C. D.; Adamson, R. D.; Furlani, T. R.; Lee, M. S.; Lee, A. M.; Gwaltney, S. R.; Adams, T. R.; Ochsner, C.; Gilbert, A. T. B.; Kedziora, G. S.; Rassolov, V. A.; Maurice, D. R.; Nair, N.; Shao, Y.; Besley, N. A.; Maslen, P. E.; Dombroski, J. P.; Daschel, H.; Zhang, W.; Korabath, P. P.; Baker, J.; Byrd, E. F. C.; Voorhis, T. V.; Oumi, M.; Hirata, S.; Hsu, C.-P.; Ishikawa, N.; Florian, J.; Warshel, A.; Johnson, B. G.; Gill, P. M. W.; Head-Gordon, M.; Pople, J. A. *J. Comput. Chem.* **2000**, *21*, 1532–1548. (b) Hehre, W. J. *A Guide to Molecular Mechanics and Quantum Chemical Calculations*; Wavefunction, Inc.: Irvine, CA 2003. (c) Hehre, W. J.; Radom, L.; Schleyer, P. v.; Pople, J. A. *Ab Initio Molecular Orbital Theory*; Wiley: New York, 1986. (d) The Spartan ‘02 Macintosh and Spartan ‘02 Unix programs are available from Wavefunction, Inc., Irvine, CA 92612.
- (17) (a) Gaussian 03, Revision A.1. Frisch, M. J.; Trucks, G. W.; Schlegel, H. B.; Scuseria, G. E.; Robb, M. A.; Cheeseman, J. R.; Montgomery, Jr., J. A.; Vreven, T.; Kudin, K. N.; Burant, J. C.; Millam, J. M.; Iyengar, S. S.; Tomasi, J.; Barone, V.; Mennucci, B.; Cossi, M.; Scalmani, G.; Rega, N.; Petersson, G. A.; Nakatsuji, H.; Hada, M.; Ehara, M.; Toyota, K.; Fukuda, R.; Hasegawa, J.; Ishida, M.; Nakajima, T.; Honda, Y.; Kitao, O.; Nakai, H.; Klene, M.; Li, X.; Knox, J. E.; Hratchian, H. P.; Cross, J. B.; Adamo, C.; Jaramillo, J.; Gomperts, R.; Stratmann, R. E.; Yazyev, O.; Austin, A. J.; Cammi, R.; Pomelli, C.; Ochterski, J. W.; Ayala, P. Y.; Morokuma, K.; Voth, G. A.; Salvador, P.; Dannenberg, J. J.;

- Zakrzewski, V. G.; Dapprich, S.; Daniels, A. D.; Strain, M. C.; Farkas, O.; Malick, D. K.; Rabuck, A. D.; Raghavachari, K.; Foresman, J. B.; Ortiz, J. V.; Cui, Q.; Baboul, A. G.; Clifford, S.; Cioslowski, J.; Stefanov, B. B.; Liu, G.; Liashenko, A.; Piskorz, P.; Komaromi, I.; Martin, R. L.; Fox, D. J.; Keith, T.; Al-Laham, M. A.; Peng, C. Y.; Nanayakkara, A.; Challacombe, M.; Gill, P. M. W.; Johnson, B.; Chen, W.; Wong, M. W.; Gonzalez, C.; Pople, J. A. Gaussian, Inc.: Pittsburgh, PA, 2003 (b) Foresman, J. B.; Frisch, A. *Exploring Chemistry with Electronic Structure Methods*, 2nd ed.; Gaussian, Inc.: Pittsburgh, PA, 1996. (c) Clark, T.; Chandrasekhar, J.; Spitznagel, G. W.; Schleyer, P. v. R. *J. Comput. Chem.* **1983**, *4*, 294.
- (18) (a) Dunning, T. H. *J. Chem. Phys.* **1989**, *90*, 1007. (b) Woon, D.; Dunning, T. H. *J. Chem. Phys.* **1993**, *98*, 1358. (c) Woon, D.; Dunning, T. H. *J. Chem. Phys.* **1995**, *103*, 4572. (d) Wilson, A.; van Mourik, T.; Dunning, Jr., T. H. *J. Mol. Struct. (THEOCHEM)* **1997**, *388*, 339.
- (19) Wiberg, K. B.; Castejon, H.; Bailey, W. F.; Ochterski, J. J. *Org. Chem.* **2000**, *65*, 1181.
- (20) Becke, A. D. *Phys. Rev.* **1988**, *A38*, 3098–3100.
- (21) Lee, C.; Yang, W.; Parr, R. G. *Phys. Rev.* **1988**, *B37*, 785.
- (22) Dirac, P. A. M. *Proc. Cam. Philos.* **1930**, *26*, 376.
- (23) Slater, J. C. *Quantum Theory of Molecules and Solids*; McGraw-Hill: New York, 1974; Vol. 4.
- (24) Vosko, S. H.; Wilk, L.; Nusair, M. *Can. J. Phys.* **1980**, *58*, 1200.
- (25) Stephens, P. J.; Devlin, F.; Chabalowski, C. F.; Frisch, M. J. *J. Phys. Chem.* **1994**, *98*, 11623.
- (26) (a) Harris, J.; Jones, R. O. *J. Phys. Chem.* **1974**, *F4*, 1170. (b) Gunnarson, O.; Lundqvist, B. I. *Phys. Rev. B* **1976**, *13*, 4274; (c) Harris, J. *J. Phys. Rev. A* **1948**, *29*, 1648.
- (27) Perdew, J. P. *Phys. Rev. B* **1986**, *33*, 8822.
- (28) Becke, A. D. *J. Chem. Phys.* **1993**, *98*, 5648.
- (29) Perdew, J. P.; Burke, K.; Wang, Y. *Phys. Rev. B* **1996**, *54*, 16533 and reference cited therein.
- (30) CCCBDB. *Vibrational Frequency Scaling Factors*; <http://srdata.nist.gov/cccdb/vsf.asp>.
- (31) Lynch, B. J.; Zhao, Y.; Truhlar, D. G. *Database of Frequency Scaling Factors for Electronic Structure Methods*, 2003; http://comp.chem.umn.edu/database/freq_scale.htm.
- (32) (a) Chambers, C. C.; Hawkins, G. D.; Cramer, C. J.; Truhlar, D. G. *J. Phys. Chem.* **1996**, *100*, 16385–16398. (b) Cramer, C. J.; Truhlar, D. G. *J. Comput. Chem.* **1992**, *13*, 1089. (c) Cramer, C. J.; Truhlar, D. G. *J. Am. Chem. Soc.* **1993**, *115*, 8810.
- (33) (a) Miertus, S.; Scrocco, E.; Tomasi, J. *Chem. Phys.* **1981**, *55*, 117. (b) Miertus, S.; Tomasi, J. *Chem. Phys.* **1982**, *65*, 239.
- (34) (a) Schlegel, H. B. *J. Comput. Chem.* **2003**, *24*, 1514–1527. (b) Ayala, P. Y.; Schlegel, H. B. *J. Chem. Phys.* **1997**, *107*, 375–384. (c) Gonzalez, C.; Schlegel, H. B. *J. Chem. Phys.* **1990**, *90*, 2154–2161. (d) Gonzalez, C.; Schlegel, H. B. *J. Phys. Chem.* **1990**, *94*, 5523–5527. (e) Peng, C.; Schlegel, H. B. *Israel. J. Chem.* **1993**, *33*, 449. (f) Peng, C.; Ayala, P. Y.; Schlegel, H. B.; Frisch, M. J. *J. Comput. Chem.* **1995**, *16*, 49.
- (35) (a) Bondi, A. *J. Phys. Chem.* **1964**, *68*, 441. (b) Pauling, L. *Nature of the Chemical Bond*, 3rd ed.; Cornell University Press: Ithaca, NY, 1960; pp 260–261. (c) Proserpio, D. M.; Hoffmann, R.; Levine, R. D. *J. Am. Chem. Soc.* **1991**, *113*, 3217. (d) Chauvin, R. *J. Phys. Chem.* **1992**, *96*, 9194. (e) O'Keeffe, M.; Brese, N. E. *J. Am. Chem. Soc.* **1991**, *113*, 3226. (f) Halgren, T. *J. Am. Chem. Soc.* **1992**, *114*, 7827. (g) Carroll, F. A. *Perspectives on Structure and Mechanism in Organic Chemistry*, Brooks/Cole: New York, 1998; pp 5–8. (h) Ma, B.; Lii, J.-H.; Schaefer, H. F., III. Allinger, N. L. *J. Phys. Chem.* **1996**, *100*, 8763–8769 and references therein. (i) Wiberg, K. B.; Murcko, M. A. *J. Comput. Chem.* **1987**, *8*, 1124–1130.
- (36) Moran, D.; Sukcharoenphon, K.; Puchta, R.; Schaefer, H. F., III; Schleyer, P. v. R.; Hoff, C. D. *J. Org. Chem.* **2002**, *67*, 9061–9069 and references therein.
- (37) Freeman, F.; Bond, D.; Keindl, M. C. Unpublished data.
- (38) (a) Xantheas, S.; Dunning, T. H., Jr. *J. Phys. Chem.* **1993**, *97*, 6616. (b) Smart, B. A.; Schiesser, C. H. *J. Comput. Chem.* **1995**, *16*, 1055. (c) Ruttkin, P. J. A.; Burgers, P. C.; Francis, J. T.; Terlouw, J. K. *J. Phys. Chem.* **1996**, *100*, 9694. (d) Frank, A. J.; Sadilek, M.; Ferrier, J. G.; Turecek, F. *J. Am. Chem. Soc.* **1997**, *118*, 11321. (e) Frank, A. J.; Sadilek, M.; Ferrier, J. G.; Turecek, F. *J. Am. Chem. Soc.* **1997**, *119*, 12343. (f) Turecek, F. *J. Phys. Chem. A* **1998**, *102*, 4703.
- (39) Freeman, F.; Cha, C. *J. Phys. Org. Chem.* **2004**, *17*, 32–41.
- (40) Freeman, F.; Cha, C. *Int. J. Quantum Chem.* **2004**, *96*, 443–455.
- (41) Tsuzuki, S.; Lüthi, H. P. *J. Chem. Phys.* **2001**, *114*, 3949–3957.
- (42) Kwiatkowski, J. S.; Leszczynski, J. *J. Mol. Struct.* **1996**, *376*, 325–342.
- (43) (a) Leszczynski, J. In *The Encyclopedia of Computational Chemistry*; Schleyer, P. v. R., Allinger, N. L., Clark, T., Gasteiger, J., Kollman, P. A., Schaefer, H. F., III, Schreiner, P. R., Eds.; Wiley: Chichester, U.K., 1998; pp 2951–2960. (b) Yekeler, H.; Ozbakir, D. *J. Mol. Model.* **2001**, *7*, 103. (c) Rueda, M.; Luque, F. J.; Lopez, J. M.; Orozco, M. *J. Phys. Chem. A* **2001**, *105*, 6575–6580. (d) Brown, R. D.; Godfrey, P. D.; McNaughton, D.; Pierlot, A. P. *J. Am. Chem. Soc.* **1989**, *93*, 2308–2310. (e) Lapinski, L.; Nowak, M. J.; Les, A.; Adamowicz, L. *J. Phys. Chem.* **1990**, *94*, 6555.
- (44) Mulliken, R. S. *J. Phys. Chem.* **1955**, *23*, 1833.
- (45) (a) Reed, A. E.; Curtiss, L. A.; Weinhold, F. *Chem. Rev.* **1988**, *88*, 899. (b) Weinhold, F.; Carpenter, J. E. *Plenum* **1988**, 227. (c) Reed, A. E.; Weinhold, F. *J. Chem. Phys.* **1986**, *84*, 2428. (d) Reed, A. E.; Weinstock, R. B.; Weinhold, F. *J. Chem. Phys.* **1985**, *83*, 735.
- (46) (a) Breneman, C. M.; Wiberg, K. B. *J. Comput. Chem.* **1990**, *11*, 361. (b) Chirlan, L. E.; Francil, M. M. *J. Comput. Chem.* **1987**, *8*, 894. (c) Wiberg, K. B.; Rablen, P. R. *J. Comput. Chem.* **1993**, *14*, 1504.
- (47) (a) Besler, B. H.; Merz, K. M., Jr.; Kollman, P. K. *J. Comput. Chem.* **1990**, *11*, 431. (b) Singh, U. C.; Kollman, P. A. *J. Comput. Chem.* **1984**, *5*, 129.
- (48) (a) Renfold, B. R. *Acta Crystallogr.* **1953**, *6*, 707. (b) Ohms, V. H.; Guth, H.; Kutoglu, A.; Scheringer, C. *Acta Crystallogr. B* **1982**, *38*, 831.
- (49) Del Bene, J. B. In *The Encyclopedia of Computational Chemistry*; Schleyer, P. v. R., Allinger, N. L., Clark, T., Gasteiger, J., Kollman, P. A., Schaefer, H. F., III, Schreiner, P. R., Eds.; Wiley: Chichester, U.K., 1998; pp 1263–1286.
- (50) (a) Crews, P.; Rodríguez, J.; Jaspers, M. *Organic Structure Analysis*, Oxford: New York, 1998. (b) Lambert, J. B.; Shurvell, H. F.; Lightner, D. A.; Cooks, R. G. *Organic Structural Spectroscopy*, Prentice Hall: Upper Saddle River, NJ 07458, 1998. (c) Silverstein, R. M.; Webster, F. X. *Spectrometric Identification of Organic Compounds*, 6th ed.; Wiley: New York, 1998.
- (51) Wiberg, K. B.; Rablen, P. R. *J. Am. Chem. Soc.* **1995**, *117*, 2201–2209.
- (52) Wiberg, K. B.; Rush, D. J. *J. Am. Chem. Soc.* **2001**, *123*, 2038–2046.
- (53) Neugebauer, C. S. M.; Taha, A. N.; True, N. S.; LeMaster, C. B. *J. Phys. Chem. A* **1997**, *101*, 4699–4706.
- (54) Chou, P.-T.; Wei, C.-Y.; Hung, F.-T. *J. Phys. Chem. B* **1997**, *101*, 9119–9126.
- (55) Close, D. M.; Crespo-Hernández, C. E.; Gorb, L.; Leszczynski, J. *J. Phys. Chem. A* **2005**, *109*, 9279–9283 and references therein.
- (56) (a) Beak, P.; Covington, J. B.; Smith, J. G.; White, J. M.; Zeigler, J. M. *J. Org. Chem.* **1980**, *45*, 1354. (b) Beak, P.; Bobham, J.; Lee, J. T. *J. Am. Chem. Soc.* **1968**, *90*, 1569.
- (57) Field, M. J.; Hillier, I. H. *J. Chem. Soc., Perkin Trans. 2* **1987**, 617–622 and references therein.
- (58) Fu, A.; Li, H.; Du, D.; Zhou, Z. *J. Phys. Chem. A* **2005**, *109*, 1468–1477.